On the instability of small gas bubbles moving uniformly in various liquids

By R. A. HARTUNIAN* and W. R. SEARS
Graduate School of Aeronautical Engineering, Cornell University, Ithaca

(*Received* 17 *May* 1957)

SUMMARY

The instability of small gas bubbles moving uniformly in various liquids is investigated experimentally and theoretically.

The experiments consist of the measurement of the size and terminal velocity of bubbles at the threshold of instability in various liquids, together with the physical properties of the liquids. The results of the experiments indicate the existence of a universal stability curve. The nature of this curve strongly suggests that there are two separate criteria for predicting the onset of instability, namely, a critical Reynolds number (202) and a critical Weber number (1·26). The former criterion appears to be valid for bubbles moving uniformly in liquids containing impurities and in the somewhat more viscous liquids, whereas the latter criterion is for bubbles moving in pure, relatively inviscid liquids.

The theoretical analysis is directed towards an investigation of the possibility of the interaction of surface tension and hydrodynamic pressure leading to unstable motions of the bubble, i.e. the existence of a critical Weber number. Accordingly, the theoretical model assumes the form of a general perturbation in the shape of a deformable sphere moving with uniform velocity in an inviscid, incompressible fluid medium of infinite extent. The calculations lead to divergent solutions above a certain Weber number, indicating, at least qualitatively, that the interaction of surface tension and hydrodynamic pressure can result in instabilities of the bubble motion.

A subsequent investigation of the time-independent equations, however, shows the presence of large deformations in shape of the bubble prior to the onset of unstable motion, which is not compatible with the approximation of perturbing an essentially spherical bubble. This deformation and its possible effects on the stability calculation are therefore determined by approximate methods. From this it is concluded that the deformation of the bubble serves to introduce quantitative, but not qualitative, changes in the stability calculation.

* Now at Cornell Aeronautical Laboratory, Buffalo, New York.

1. Introduction

Very small bubbles rise in a rectilinear path in a body of liquid at rest. It is found, however, that if one forms larger bubbles in liquids of relatively small viscosity, a critical size for each liquid is reached at which the bubble suddenly assumes an oscillatory trajectory. The actual path is most often helical, although the bubble is occasionally seen to oscillate in a single plane as it rises. The bubbles in this region are seen to be slightly deformed; they seem to have the shape of oblate spheroids. Still larger bubbles become more deformed and rise rectilinearly, but with a rocking motion about the axis in the direction of their motion. Finally, a size is reached at which the bubble rises rectilinearly maintaining a spherical shape on its upper surface but a very irregular, fluctuating shape on its lower surface. These bubbles have been called 'spherical-cap' bubbles. For more viscous liquids, such as mineral oil, the bubbles simply become more and more deformed as the size is increased, with no oscillations in shape. Accordingly, all bubbles in such liquids rise rectilinearly.

It is the purpose of this paper to examine experimentally the conditions necessary for the onset of oscillations in relatively inviscid liquids, and to develop a theory to predict these 'critical' conditions.

Most of the previous theoretical research has been limited to solutions for the drag of rigid and fluid spheres moving slowly and uniformly in an infinite medium. Usually, the inertial terms in the Navier–Stokes equations have been neglected. Notable exceptions to this trend of research are the solutions for the shape and motion of spherical-cap bubbles by Davies & Taylor (1950), and for the drag of rigid spheres at a Reynolds number of about 100 by Kawaguti (1955). Kawaguti studied the stability of the flow about spheres and found instability at a Reynolds number of 51, which is approximately one-half of the observed value for rigid spheres. His treatment is not applicable to fluid spheres because of the slip boundary condition required. Recently, Saffman (1956) obtained relations for the terminal velocities of spiralling bubbles in water by assuming the flow near the front of the bubble to be inviscid and considering the distribution of pressure in the vicinity of the stagnation point. By treating the planar oscillating bubbles in the same way, he arrived at an equation which determines the stability of the rectilinear motion of bubbles in water. The value of the critical Weber number $U(\rho r_e/T)^{1/2}$ deduced by this method is at variance with experimental results by a factor of two. (Here U denotes the speed at which the bubble rises, ρ the density of the liquid, r_e the equivalent radius $(3 \times \text{volume}/4\pi)^{1/3}$ of the bubble, and T the surface tension.)

Rayleigh solved the problem of the oscillation of a liquid or gaseous sphere at rest in an infinite medium otherwise at rest (see Lamb 1932, p. 473). The more general solution for the oscillations of a gaseous sphere moving with a uniform velocity U in an infinite medium, to be obtained in the ensuing sections, reduces to Rayleigh's result when U is equated to zero.

There has been a considerable amount of experimental investigation on the rates of rise of bubbles in various liquids (Hoefer 1913; Miyagi 1925; Bryn 1949; Datta *et al.* 1950; etc.). Rosenberg (1950) and particularly Haberman & Morton (1953) have conducted by far the most systematic experiments covering the spectrum of most of the pertinent variables. The latter have also made an exhaustive study of the literature, collating the data of the previous experimenters and integrating these data with their own. Rosenberg improved the experimental technique and repeated the experiments on the rate of rise of air bubbles in water over a wide range of bubble sizes. He suggested the use of the three dimensionless parameters: drag

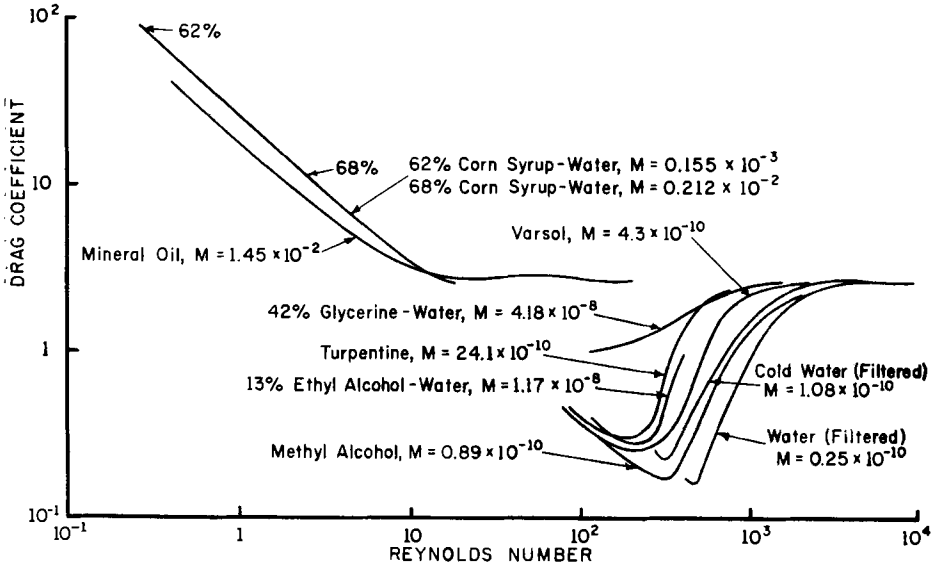

Figure 1. Drag coefficient as a function of Reynolds number for ellipsoidal and spherical-cap bubbles in various liquids. (Courtesy of David Taylor Model Basin, Navy Department.)

coefficient $C_D = (8/3)(gr_e/U^2)$, Reynolds number $Re = 2\rho U r_e/\mu$, and a third parameter $M = g\mu^4/\rho T^3$ for the description of bubble motion in liquids. Here g denotes the acceleration due to gravity and μ the coefficient of viscosity. Haberman & Morton, using the same experimental technique as Rosenberg, investigated the effect of variation of liquid properties on the motion of air bubbles and also made an experimental evaluation of the wall effect. They used eleven fluids with different properties (the same fluid at different temperatures being considered to be a new fluid) and three tanks of varying dimensions. In an attempt to correlate their data, they plotted their results in terms of the basic dimensionless parameters cited above. Figure 1 gives the experimental results in terms of the drag coefficient, Reynolds number and M, whereas in figure 2, the data are presented in terms of the

drag coefficient, the Weber number and M. Examination of these curves indicates that there is no completely systematic arrangement with changes in M. Accordingly, it can be concluded that the variables considered in these non-dimensional parameters are insufficient for a complete description of bubble motion. Nevertheless, there is a definite trend towards categorizing the bubbles in groups according to the values of M. Figure 2 shows good correlation among the 'fast' fluids ($M = 10^{-10}$ to 10^{-8}) and sets a clear distinction between these fluids and the 'slow' fluids ($M = 10^{-7}$ to 10^{-2}). This paper is mainly concerned with the 'fast' fluids.

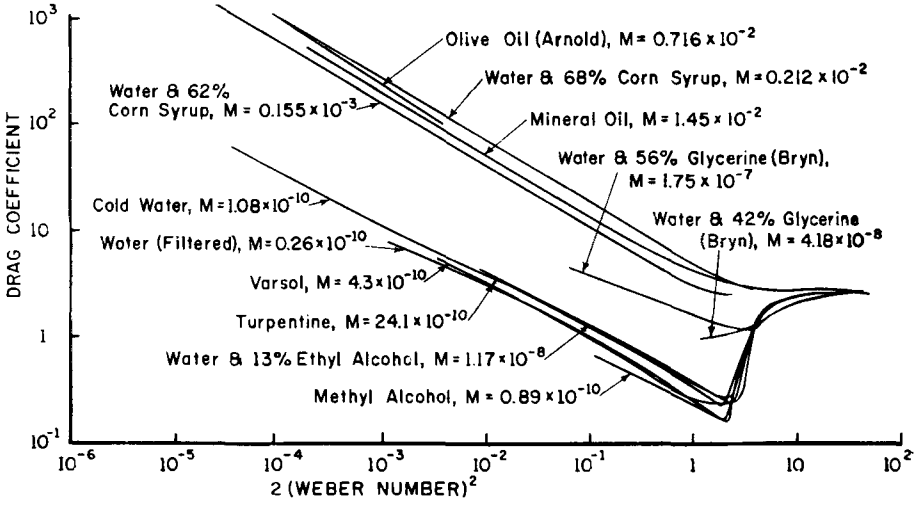

Figure 2. Drag coefficient as a function of Weber number for air bubbles rising at their terminal velocity in various liquids. (Courtesy of David Taylor Model Basin, Navy Department.)

In examining the two plots, it is seen that the minimum drag attained by bubbles in various test liquids occurs at different Reynolds numbers, but at essentially the same Weber number (1·0 to 1·3). The correlation of all the curves for the 'fast' fluids above a Weber number of about 1·3 indicates the importance of hydrodynamic and surface-tension forces in this range.

2. Experiments

The experimental study was conducted to ascertain a conjecture of Professor von Kármán that the Weber number should be a significant parameter involved in the stability of gas bubbles rising in liquids. Accordingly, measurements of the size and terminal velocities of bubbles which just become unstable were made in twelve liquids. In addition, the physical properties of the liquids were measured.

Figure 3 (plate 1) is a photograph of the experimental arrangement. The cylindrical tube is 5·7 cm in diameter, which is sufficient to make any wall effect negligible. The bubble-generating device consists of a *T*-section made of capillary tubing of uniform bore (0·7 mm inside diameter) and two rubber syringes. This is a modification of the system employed by Saffman (1956). A shop microscope was used to measure the length (from which the equivalent radius is calculated) of small bubbles formed in the vertical section of the *T*-shaped capillary. Fine black thread tied about the tube at two points a known distance apart (50·2 cm) provided the distance markings for the velocity measurements. These were placed within the region where the bubbles had attained their terminal velocities. The time taken for the bubbles to traverse this distance was measured by means of a stop watch. This measurement is the least accurate in the experiment. An estimate of the accuracy attainable is approximately 5% for the more rapidly moving bubbles. The viscosity of the liquids was measured by means of an Ostwald viscometer, and the surface tension by a DuNuoy tensiometer. The density of each liquid at the appropriate temperature was obtained from the *Handbook of Chemistry and Physics*.

The experimental procedure consisted first of measuring the physical properties of the test liquid. Air was bubbled freely through the liquid in order to reduce any tendency towards diffusion through the bubble surface. A single bubble was then formed in the vertical section of the capillary *T* by applying pressure to the syringe containing air until the desired quantity of air had penetrated the liquid in the vertical section of the *T*, at which time the syringe containing the test liquid was squeezed, thus cutting off the desired volume of air. By continued pressure on the latter syringe, the bubble could be made to advance up the capillary tube to a point where its length was measured by the shop microscope (or a rule with fine divisions, for larger bubbles). Following this operation, the bubble was forced into the fluid medium at the orifice and carefully released from the orifice. The time taken for it to cross the markings was measured. Allowing sufficient time for the wake effects of the previous bubble to be dissipated, another bubble was formed and the process repeated. Starting with small bubbles and forming successively larger ones, a 'critical' size was found for each liquid at which the bubble would just begin to oscillate. Many bubbles formed about this size then made possible a better determination of the critical conditions for each liquid. Upon completion of the test for a given liquid, a second temperature reading was taken, and, if any difference from the initial reading was detected, the physical properties of the liquids were obtained by interpolation from tables using the average temperature.

From estimates of the experimental accuracy of the individual measurements, it is expected that probable errors of the order of 10% may occur in the calculation of the critical Reynolds and Weber numbers from the data. It is clear from this fact that only significant trends were being sought from these experiments.

Since it has been found that slight concentrations of impurities in liquids have profound effects on the motion of gas bubbles through them (Gorodetskaya 1949; Stuke 1952), great care was exercised in ascertaining the purity of the test liquids. Figure 4 compares the drag coefficients of bubbles in water containing slight concentrations of surface-active substances with those in filtered water. Tap water and test liquids obtained from ordinary storage drums were found to behave in a manner analogous to water containing surface-active substances. The drag coefficient in the impure liquids is seen to follow the curve for rigid spheres up to a Reynolds number of 200 or so. Of particular importance is the fact that the drag coefficient of bubbles in pure liquids is considerably smaller than that in the impure liquids.

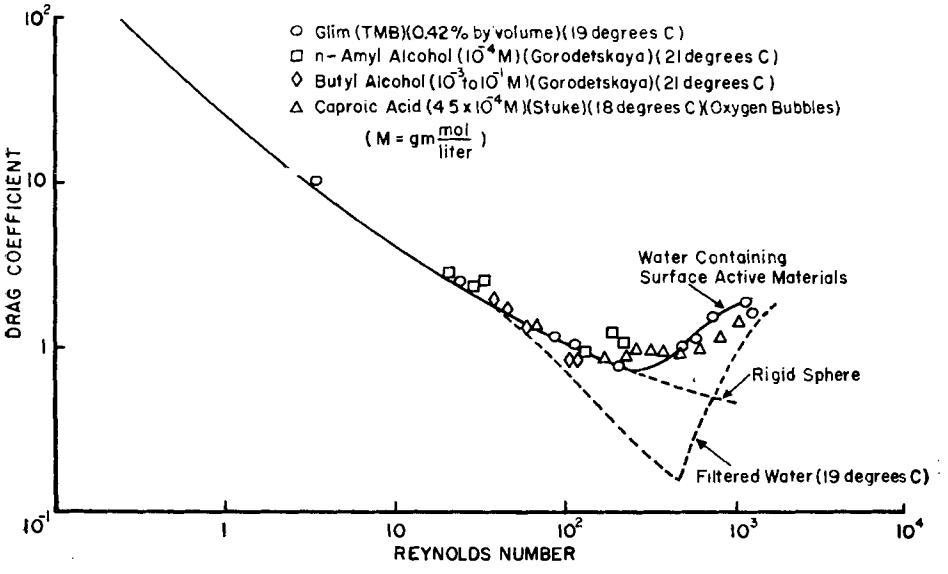

Figure 4. Drag coefficient as a function of Reynolds number for bubbles rising at their terminal velocity in water containing various surface-active materials. (Courtesy of David Taylor Model Basin, Navy Department.)

Aside from the criterion of purity, an attempt was made to select different liquids with some similar physical properties. For example, methyl alcohol and ethyl alcohol have essentially the same surface tension and density, but radically different viscosities.

Since the experiments were designed to reveal the significance of the Weber number in determining the instability of bubbles, liquids of relatively low viscosity were selected to reduce the role played by the Reynolds number. Indeed, as discussed in a previous section, bubbles rising in very viscous liquids (roughly, $M \geqslant 10^{-4}$) do not become unstable.

From the experimental determination of the critical bubble size and terminal velocity, as well as the properties of the various liquids, the *critical*

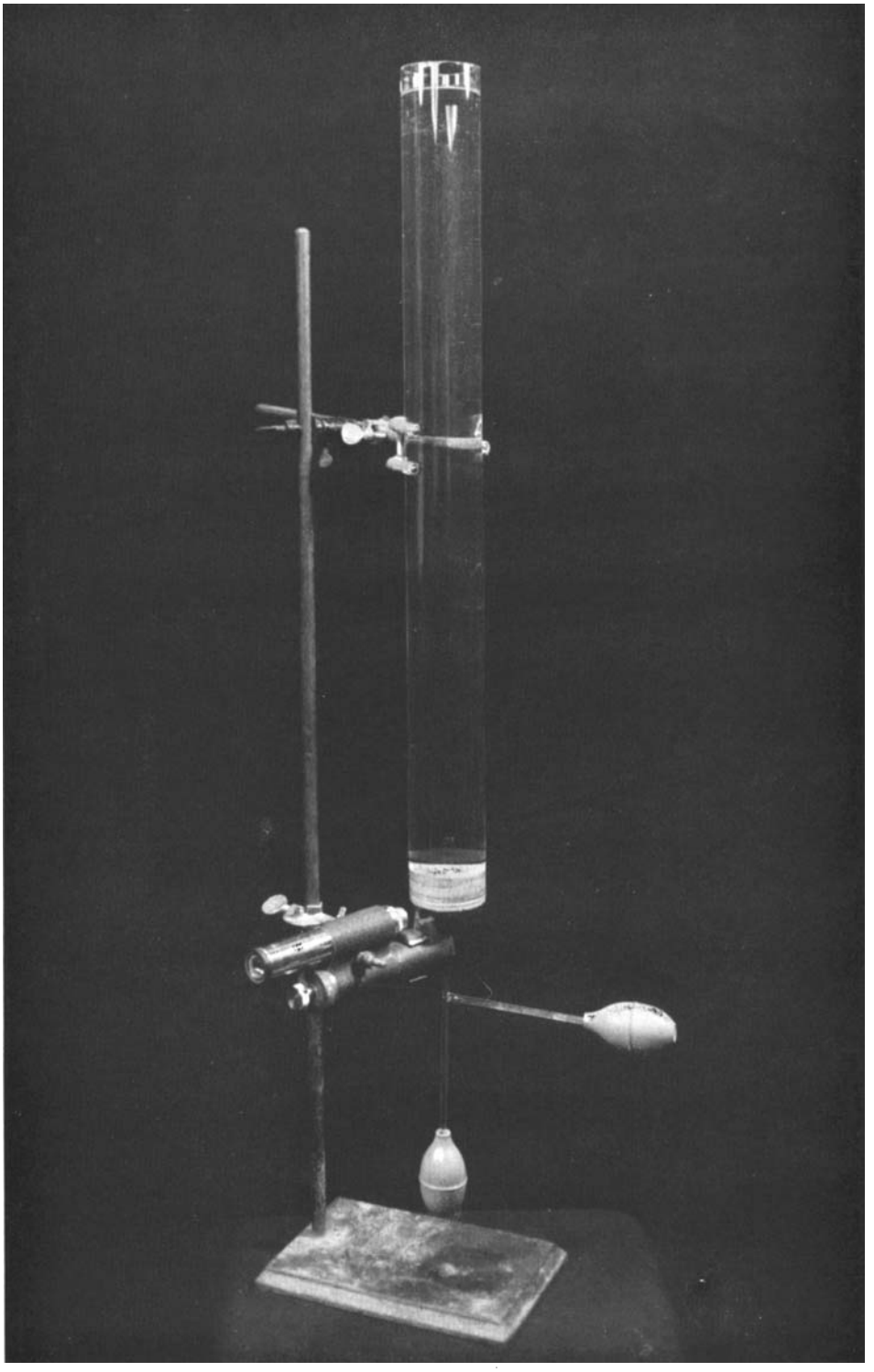

Figure 3. Photograph of experimental arrangement.

Liquid	Temp (° C)	Critical radius (cm)	Terminal velocity (cm/sec)	Critical Reynolds number	Critical Weber number	Critical Bond number	Critical Froude number
1. Methyl Alcohol	21·1	0·067	26·6	475	1·25	2·60	10·6
2. Distilled water	24·5	0·085	35·5	670	1·22	3·18	15·1
3. CCL_4 (Pure)	23·0	0·056	26·3	486	1·32	2·68	12·5
4. Ethyl alcohol	23·0	0·084	26·0	286	1·33	2·15	8·2
5. Benzene	21·0	0·062	28·9	474	1·24	2·98	13·7
6. Impure distilled water	24·5	0·065	15·4	214	0·489	3·94	3·72
7. Impure CCL_4	23·0	0·044	15·2	190	0·675	2·98	4·05
8. Tap water	22·5	0·063	15·4	206	0·484	4·05	3·84
9. Hot tap water	43·0	0·049	14·0	214	0·402	5·01	4·07
10. 20% (wt.) glycerol	23·0	0·076	17·6	176	0·601	3·37	4·13
11. 30% (wt.) glycerol	22·0	0·091	21·6	183	0·814	2·81	5·20
12. 40% (wt.) glycerol	23·5	0·110	27·8	200	1·19	2·24	7·10
13. Filtered water (Haberman & Morton)	19·0	0·070	34·0	475	1·05	2·55	16·9
14. Filtered water (Haberman & Morton)	6·0	0·085	31·0	355	1·05	3·22	11·4
15. Filtered water (Rosenberg)	19·0	0·077	34·0	522	1·11	2·82	15·4
16. Water (Miyagi)		0·165	27·8	1020	1·35	1·64	4·91
17. Distilled water (oxygen bubbles, Stuke)	18·0	0·085	35·5	602	1·21	3·21	15·1
18. Varsol (Haberman & Morton)	28·0	0·070	25·5	330	1·20	2·51	9·68
19. Turpentine (Haberman & Morton)	23·0	0·115	22·5	306	1·34	1·58	4·50
20. Methyl Alcohol (Haberman & Morton)	30·0	0·060	25·0	450	1·16	2·81	11·0
21. Tap water (Haberman & Morton)	21·0	0·065	16·0	202	0·479	4·19	4·02
22. Hot tap water (Haberman & Morton)	49·0	0·050	13·0	232	0·350	5·32	3·45

Table 1. Bubble size, terminal velocity, and non-dimensional parameters at critical conditions.

Reynolds, Weber, Bond $r_e(\rho g/T)^{1/2}$ and Froude U^2/gr_e numbers were calculated (table 1). The values obtained by other experimenters are also listed. Figure 5 is a plot of these results in terms of the Weber number and Reynolds number. The average curve drawn through the experimental points is seen to give the strong indication that there are two distinct criteria for determining the onset of instability in gas bubbles rising in liquids of relatively low viscosity. There is one branch of the curve that is independent of the Weber number, with the average value of 202 for the Reynolds number, whereas the other branch (at $Re > 202$) is independent of the Reynolds number and has the average value of 1·26 for the Weber number.

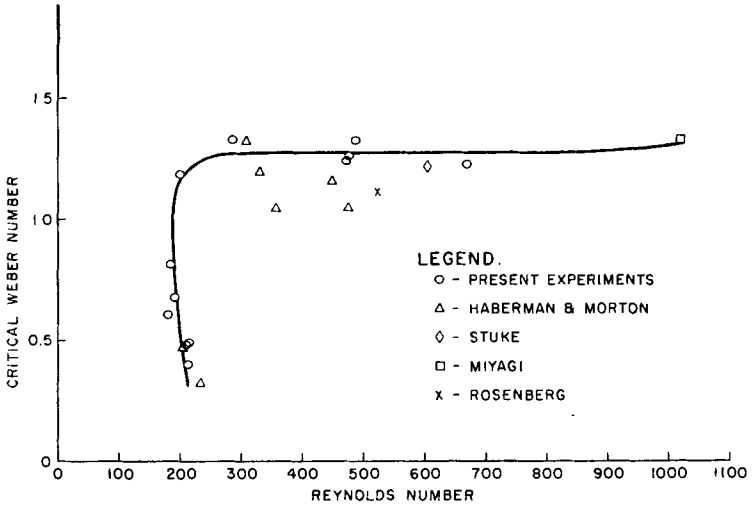

Figure 5. Stability curve (critical Weber number as a function of Reynolds number for various liquids).

It seems significant that the former branch is made up not only of the more viscous liquids but also the impure ones. This may be taken as added evidence that impurities affect particularly the conditions at the surface of the bubble, introducing, it would seem, an increased apparent viscosity.

When the nature of the stability curve became known, an experimental technique was developed to shed further light on the distinction between the two types of instabilities. Vegetable dye was added to the liquid in the syringe attached to the vertical section of the bubble-generating device (figure 3). By carefully forming a bubble, it was possible to see a closed wake behind a stable bubble as it rose. By closer examination, the dye could be seen to be rolled up into a vortex ring symmetrically situated with respect to the bubble. It is significant that the wake could be seen only in the impure and more viscous liquids. When the bubble size was increased to give critical conditions, the bubble oscillated and the wake dispersed. When this same experiment was attempted with distilled water, the following

sequence of events was seen to occur: (*a*) as the bubble left the orifice, the dye formed a closed wake; (*b*) after rising an inch or so, the bubble oscillated several times and shed the wake; (*c*) upon shedding the dye, it rose uniformly and rectilinearly; and (*d*) if the bubble size at the orifice was just below the critical size for distilled water, it would begin to oscillate before it had reached the surface. A possible explanation of this behaviour is as follows: (*a*) the presence of the dye in the otherwise pure liquid tended to transform its characteristics to those of the impure liquids; (*b*) in accelerating from rest at the orifice to the terminal velocity for distilled water, the bubble had to pass through the 'critical Reynolds number' (202), and since it possessed the properties of an impure liquid, the bubble oscillated enough to shed its wake; (*c*) with the dye shaken from the surface of the bubble, the impurities were in effect removed, so that the bubble returned to its normal course in the pure water, i.e. it rose rectilinearly; and finally, (*d*) since the Weber number of a bubble increases (slightly) as it rises, owing to the reduction of the hydrostatic pressure and subsequent increase in volume (and therefore velocity), a bubble which was just sub-critical at the orifice might become critical as it rose. Fairly conclusive evidence regarding the action of the dye as an impurity is provided by the fact that if no dye was added to the liquid the short oscillation an inch or so above the orifice was never observed. The experiment described above seems to support the existence of two different types of instability, both observable with one bubble.

Referring back to figure 2, it is seen that the minimum drag for bubbles in liquids with small values of M occurs at a fairly universal value of the Weber number. In addition, the value of this Weber number is in agreement, within the limits of accuracy, with the experimentally determined critical Weber number for oscillations, i.e. 1·26. The fact that the minimum drag coefficient and the onset of oscillation of the bubbles occur at almost the same Weber number is construed by the authors as providing additional evidence for the existence of a critical Weber number, since the oscillatory trajectory would contribute substantially to the observed rapid increase in drag with increasing Weber number beyond the critical value. Of course, the deformation of the bubbles at these Weber numbers is also a contributing factor to the increase in drag.

The stability curve (figure 5) is not quite analogous to the familiar stability diagrams in which a curve separates regions of stability from regions of instability. The actual meaning of the present stability curve is that for any liquid capable of producing unstable bubbles, the critical Weber number and critical Reynolds number must be such as to fit somewhere on this curve. Indeed, bubbles rising at Reynolds numbers less than 202 in Reynolds-number-dependent liquids are invariably stable, independent of the value of the Weber number, while bubbles rising in pure, relatively inviscid liquids at Reynolds numbers greater than 202 remain stable until they attain the value of the critical Weber number.

From table 1, it may be seen that there is no systematic variation of the Bond number with the Reynolds number at critical conditions, but that the critical Froude number increases fairly regularly with increasing Reynolds number. The latter result may have been expected, since the Froude number is inversely proportional to the drag coefficient. That the high values of the Foude number occur for liquids which have the Weber number as a stability criterion corroborates the contention that instability in these liquids begins at low drag coefficients (actually, almost minimum drag).

The duality of cause for instability is not peculiar to bubbles rising in liquids. Similar results have been observed in investigations on the stability of liquid jets issuing from circular orifices (Richardson 1950, p. 100). It has been noted that falling drops break up at a critical value of the Weber number (Lane & Green 1956, pp. 186–192).

The following conclusions are drawn from the present experimental results.

1. A universal stability curve which determines the critical conditions necessary for the onset of oscillations of bubbles in most common liquids appears to exist.

2. The character of this curve strongly suggests that there are two distinct criteria for instability:

(*a*) a critical Reynolds number (202) for the impure and somewhat more viscous liquids;

(*b*) a critical Weber number (1·26) for pure, relatively inviscid liquids.

3. There is no exact method for determining which of the two criteria will prevail in a given liquid. For the pure liquids, a fairly good requirement that the Weber number be dominant is that the M number should have a value less than 10^{-9}. Unfortunately, the significant properties of 'impure' liquids do not seem to be reflected in their values of M, so that the liquids falling into this category can be identified only by experience. This implies that the important properties affected by impurities are not simply viscosity and surface tension, at least as these are usually measured.

3. Theory

In this section the stability of a deformable sphere in an inviscid, incompressible, irrotational, uniform flow to a general small perturbation in shape is calculated. In applying the results to the bubble problem, it is assumed that the hydrodynamic pressure and surface tension represent the most significant effects. The results indicate the possibility of small, high-frequency oscillations of the bubble at the lower Weber numbers, and divergence of the solution at Weber numbers above a critical value,

It will be argued that the region of small oscillations, when the damping effects of viscosity are taken into consideration, represents a stable motion of the bubble, whereas the divergent solutions actually imply the observed unstable motion.

However, a subsequent investigation of the time-independent equations shows the existence of large deformations of the bubble prior to the onset of the unstable motion, which is not compatible with the approximation of perturbing an essentially spherical bubble. This deformation and its possible effects on the stability calculation are then determined by approximate methods. From this, it is concluded that the deformation of the bubbles serves to introduce quantitative, but not qualitative, changes in the stability calculation.

This approach to the problem differs significantly from that employed by Saffman (1956) in two respects. Firstly, it is assumed that the flow about the *entire* sphere is essentially inviscid, and secondly, in addition to that mode which represents a lateral velocity perturbation, changes in shape of the bubble surface are considered to be important.

A. *Theoretical assumptions and development of the boundary condition*

The theoretical analysis is concerned only with the instability of bubbles due to hydrodynamic pressure and surface-tension effects. The correlation obtained for the critical conditions in the pure liquids with M less than 10^{-9} in terms of the Weber number (figure 5) gives significant evidence of the primary roles played by the hydrodynamic pressure and surface tension in the instability. That viscous effects are relatively unimportant in this phenomenon is, at first sight, somewhat surprising, considering the low Reynolds numbers encountered. However, the drag coefficient of the bubbles just prior to the onset of oscillations is approximately one-fifth that of a rigid sphere at the same Reynolds number. In fact, rigid spheres do not attain such low drag coefficients until Reynolds numbers of the order of 4×10^5 are reached. At these Reynolds numbers the pressure distribution about the sphere is essentially that obtained from potential theory. On the basis of this evidence, the theoretical model will have the form of a deformable sphere moving uniformly in an inviscid, incompressible fluid of infinite extent.

Gravitational forces and the pressure of the gas within the sphere due to perturbations in the shape of the sphere will be neglected. Their effects may be shown to be much smaller than those of surface tension and hydrodynamic pressure for the size bubbles considered ($r_e < 0{\cdot}09$ cm).

Since the bubbles do not change volume appreciably as they rise, the perturbation of shape will be performed so as to maintain constant volume.

Employing the usual spherical coordinates with the origin situated at the centre of the bubble, the equation for the surface of the bubble is denoted by

$$R(\theta, \phi, t) = R_0 + \sum_{n=1}^{\infty} A_n(t) S_n(\theta, \phi), \tag{1}$$

where R_0 is the equilibrium radius of the bubble, $A_n(t)$ are small time-dependent quantities such that their squares may be neglected, and the $S_n(\theta, \phi)$ are spherical surface harmonics represented by

$$S_n(\theta,\phi) = c_0 P_n(\cos\theta) + \sum_{m=1}^{\infty} (c_m \cos m\phi + d_m \sin m\phi) P_n^m(\cos\theta). \tag{2}$$

In order to maintain constant volume $A_0(t)$ is taken to be zero; thus the sum in equation (1) starts with $n = 1$. Let

$$A_n(t) = a_n e^{\lambda t} \tag{3}$$

where the coefficients a_n are small (compared to R_0) complex quantities, and λ is a complex number to be determined. If the real part of λ is negative, the ensuing motion is stable, whereas positive values of λ will indicate a divergence of the mode in question. The surface of the perturbed bubble may accordingly be represented by the equation

$$F(R,\theta,\phi,t) = R_0 + e^{\lambda t} \sum_{n=1}^{\infty} \sum_{m=0}^{n} a_{nm} P_n^m \cos m\phi - R = 0, \tag{4}$$

where it is understood that the argument of the P_n^m is $\cos\theta$ throughout the analysis. The boundary condition at the surface of the bubble may be derived from the condition

$$DF/Dt = 0, \tag{5}$$

where D/Dt is the usual convective derivative. Since we are assuming potential flow about the sphere, the velocity components at the surface of the perturbed sphere are of the forms

$$v_\theta = \tfrac{3}{2} U \sin\theta + v_\theta' + O(a_{nm}^2), \qquad v_r = v_r' + O(a_{nm}^2), \qquad v_\phi = v_\phi' + O(a_{nm}^2), \tag{6}$$

where the primes denote quantities of the first order in the perturbation amplitudes a_{nm}. If equations (4) and (6) are substituted into (5), the boundary condition on the surface of the perturbed bubble is obtained, to first order, as

$$[v_r]_R = \lambda e^{\lambda t} \sum_{n=1}^{\infty} \sum_{m=0}^{n} a_{nm} P_n^m \cos m\phi + \\ + \frac{3}{2}\frac{U}{R_0} e^{\lambda t} \sum_{n=1}^{\infty} \sum_{m=0}^{n} a_{nm} \left[\frac{n(n-m+1)}{2n+1} P_{n+1}^m - \frac{(n+1)(n+m)}{2n+1} P_{n-1}^m \right] \cos m\phi, \tag{7}$$

where use has been made of the recurrence relation for $\sin\theta\, dP_n^m/d\theta$ (Morse & Feshbach 1953, p. 1326).

In the following section, a potential will be designed to satisfy the boundary condition given by (7), and from this potential the hydrodynamic pressure will be calculated.

B. *Development of the solution*

The velocity potential must satisfy $\nabla^2\Phi = 0$. The potential may be written as

$$\Phi = -\tfrac{1}{2} U(2r + R_0^3/r^2)\cos\theta + \Phi', \tag{8}$$

where Φ' contains terms of the first order only, and the first term is the familiar velocity potential for the flow about a sphere of radius R_0. Aside from the first-order terms in (7), it is seen that the first term in (8) also contributes a first-order term in the radial component of the velocity when it is evaluated on the surface of the perturbed sphere, for

$$[v_r]_R = [v_r]_{R_0} + \left[\frac{\partial v_r}{\partial r}\right]_{R_0} \Delta R = -3\frac{U}{R_0}\cos\theta\, e^{\lambda t}\sum_{n=1}^{\infty}\sum_{m=0}^{n} a_{nm} P_n^m \cos m\phi. \quad (9)$$

Therefore, in addition to finding a potential which will satisfy equation (7), the potential must also cancel the contribution indicated in (9). If use is made of the recurrence relation for $\cos\theta P_n^m$, equation (9) may be rewritten

$$[v_r]_R = -3\frac{U}{R_0} e^{\lambda t}\sum_{n=1}^{\infty}\sum_{m=0}^{n} a_{nm}\left[\frac{(n-m+1)}{(2n+1)} P_{n+1}^m + \frac{(n+m)}{(2n+1)} P_{n-1}^m\right]\cos m\phi. \quad (10)$$

If one subtracts (10) from (7), an equivalent boundary condition remains to be satisfied, viz.

$$[v_r]_R = \lambda e^{\lambda t}\sum_{n=1}^{\infty}\sum_{m=0}^{n} a_{nm} P_n^m \cos m\phi + \frac{3}{2}\frac{U}{R_0} e^{\lambda t}\sum_{n=1}^{\infty}\sum_{m=0}^{n} a_{nm} \times$$
$$\times\left[\frac{(n+2)(n-m+1)}{2n+1} P_{n+1}^m - \frac{(n-1)(n+m)}{2n+1} P_{n-1}^m\right]\cos m\phi. \quad (11)$$

The appropriate velocity potential is seen to be

$$\Phi = -\left\{\frac{U}{2}\left(2r + \frac{R_0^3}{r^2}\right)\cos\theta + \lambda e^{\lambda t}\sum_{n=1}^{\infty}\sum_{m=0}^{n}\frac{a_{nm} R_0^{n+2}}{(n+1)r^{(n+1)}} P_n^m \cos m\phi + \right.$$
$$+ \frac{3}{2}\frac{U}{R_0} e^{\lambda t}\sum_{n=1}^{\infty}\sum_{m=0}^{n} a_{nm} \times$$
$$\left.\times\left[\frac{(n-m+1)}{2n+1}\frac{R_0^{n+3}}{r^{n+2}} P_{n+1}^m - \frac{(n-1)(n+m)}{(2n+1)nr^n} R_0^{n+1} P_{n-1}^m\right]\cos m\phi\right\}. \quad (12)$$

The pressure is calculated from

$$p/\rho + \tfrac{1}{2}v^2 + \partial\Phi/\partial t = \text{constant}. \quad (13)$$

Inasmuch as a first-order theory is being constructed, it is clear that the velocity components v_r and v_ϕ will not contribute to the fluid pressure, since each is already of the first order in a_{nm}. The velocity component v_θ, on the other hand, is, from (12),

$$[v_\theta]_R = [v_\theta]_{R_0} + \left[\frac{\partial v_\theta}{\partial r}\right]_{R_0}\Delta R + \frac{1}{R_0}\frac{\partial\Phi'}{\partial\theta}$$
$$= \frac{3}{2}U\sin\theta - \frac{3}{2}\frac{U}{R_0} e^{\lambda t}\sum_{n=1}^{\infty}\sum_{m=0}^{n} a_{nm}\sin\theta P_n^m\cos m\phi + \frac{1}{R_0}\frac{\partial\Phi'}{\partial\theta}, \quad (14)$$

so that

$$-\frac{[v_\theta^2]_R}{2} = -\frac{9}{8}U^2\sin^2\theta +$$
$$+\frac{9}{4}\frac{U^2}{R_0} e^{\lambda t}\sum_{n=1}^{\infty}\sum_{m=0}^{n} a_{nm}\sin^2\theta P_n^m\cos m\phi - \frac{3}{2}\frac{U}{R_0}\sin\theta\frac{\partial\Phi'}{\partial\theta}, \quad (15)$$

where terms of the first order only have been retained. If use is made of

the recurrence relation for $\sin^2\theta P_n^m$ (Morse & Feshbach 1953, p. 1326), it can be shown, after some algebra, that the fluid pressure as calculated from (13) is

$$\left[\frac{p}{\rho}\right]_R = \frac{p_\infty}{\rho} + \frac{U^2}{2} - \frac{9}{8}U^2\sin^2\theta + \frac{9}{4}\frac{U^2}{R_0}e^{\lambda t}\sum_{n=1}^{\infty}\sum_{m=0}^{n} a_{nm}\left\{\left[\frac{(n+m+1)(n+m+2)}{(2n+1)(2n+3)} + \right.\right.$$
$$+ \frac{(n-m-1)(n-m)}{(2n-1)(2n+1)} - \frac{(n-m+1)(n+2)(n+m+1)}{(2n+1)(2n+3)} -$$
$$\left.- \frac{(n-1)^2(n^2-m^2)}{n(2n+1)(2n-1)}\right] P_n^m -$$
$$- \left[\frac{(n-m+1)(n-m+2)}{(2n+1)(2n+3)} - \frac{(n-m+1)(n+1)(n-m+2)}{(2n+1)(2n+3)}\right] P_{n+2}^m -$$
$$\left.- \left[\frac{(n+m)(n+m-1)}{(2n+1)(2n-1)} - \frac{(n-1)(n+m)(n+m-1)}{(2n+1)(2n-1)}\right] P_{n-2}^m\right\}\cos m\phi -$$
$$- \frac{3}{2}U\lambda e^{\lambda t}\sum_{n=1}^{\infty}\sum_{m=0}^{n} a_{nm}\left[\frac{(n+m)}{2n+1}P_{n-1}^m - \frac{n(n-m+1)}{(n+1)(2n+1)}P_{n+1}^m\right]\cos m\phi +$$
$$+ \lambda^2 e^{\lambda t}\sum_{n=1}^{\infty}\sum_{m=0}^{n}\frac{a_{nm}R_0}{n+1}P_n^m\cos m\phi + \frac{3}{2}U\lambda e^{\lambda t}\sum_{n=1}^{\infty}\sum_{m=0}^{n} a_{nm}\times$$
$$\times\left[\frac{(n-m+1)}{2n+1}P_{n+1}^m - \frac{(n-1)(n+m)}{n(2n+1)}P_{n-1}^m\right]\cos m\phi, \quad (16)$$

where the terms $\partial\Phi/\partial t$ and $\partial\Phi'/\partial(\cos\theta)$ were calculated from (12).

The action of surface tension at an interface between two fluids is to cause a discontinuity in the pressure across the surface, given by the relation,

$$p_i - p = T(1/R_1 + 1/R_2), \quad (17)$$

where T is the surface tension, and R_1 and R_2 are the principal radii of curvature, considered positive if the centres of curvature lie on the side to which the subscript i refers. For the perturbed sphere in the present problem, the following form for the sum of the curvatures, correct to first order, has been derived in Lamb (1932, p. 474),

$$\frac{1}{R_1} + \frac{1}{R_2} = \frac{2}{R_0} + e^{\lambda t}\sum_{n=2}^{\infty}\sum_{m=0}^{n}\frac{(n-1)(n+2)}{R_0^2}a_{nm}P_n^m\cos m\phi. \quad (18)$$

Substituting (16) and (18) into equation (17), one has for the equilibrium of the pressure terms that are independent of time,

$$p_i = p_\infty + \frac{\rho U^2}{2} - \frac{9}{8}\rho U^2\sin^2\theta + \frac{2T}{R_0} + p'_{\lambda=0,\,m=0} + \tau'_{\lambda=0,\,m=0}, \quad (19)$$

where the last two terms refer to the first-order fluid pressure and surface-tension stresses which are time-independent and symmetric with respect to the direction of motion. Equation (19) permits calculation of the deformation of the bubble as a function of the Weber number, which will be considered in a later section. For the equilibrium of the time-dependent

pressures terms at the surface of the bubble, one has

$$\frac{9}{4}W^2a_{n+2,m}\frac{(n+m+2)(n+m+1)n}{(2n+3)(2n+5)}-\frac{3}{2}W\lambda' a_{n+1,m}\frac{(n+m+1)(2n+1)}{(n+1)(2n+3)}+$$
$$+\frac{9}{4}W^2a_{n,m}\left[\frac{(n+m+1)(n+m+2)}{(2n+1)(2n+3)}+\frac{(n-m-1)(n-m)}{(2n-1)(2n+1)}-\right.$$
$$\left.-\frac{(n-m+1)(n+2)(n+m+1)}{(2n+1)(2n+3)}-\frac{(n-1)^2(n^2-m^2)}{n(2n-1)(2n+1)}\right]+$$
$$+a_{n,m}\left[\frac{\lambda'^2}{n+1}+(n-1)(n+2)\right]+$$
$$+\frac{3}{2}W\lambda' a_{n-1,m}\frac{(n-m)}{n}+\frac{9}{4}W^2a_{n-2,m}\frac{(n-m-1)(n-m)(n-2)}{(2n-1)(2n-3)}=0, \quad (20)$$

where the conditions of orthogonality of the associated Legendre functions and the trigonometric functions have been employed, $\lambda' \equiv \lambda(\rho R_0^3)^{1/2}/T^{1/2}$, and W denotes the Weber number. The ranges of n and m are $n \geqslant 0$ and $0 \leqslant m \leqslant n$, and the a_n for $n \leqslant 0$ are considered to be zero. That this equation should be equated to zero follows from the neglect of the perturbation pressures of the gas within the bubble. For the case of zero forward velocity ($U = 0$), equation (20) reduces to the result obtained by Rayleigh, viz.

$$\lambda^2 = -\frac{(n+1)(n-1)(n+2)}{\rho R_0^3}T. \quad (21)$$

It is clear that for this case there is no coupling of the modes, or otherwise stated, the coordinate system selected for the problem consists of the normal coordinates. Therefore, it is seen that the effect of a uniform translation of the bubble is, effectively, to couple the possible modes of oscillation, or at least the modes dependent upon θ (i.e., the indices n). In seeking solutions to (20) for the stability parameter λ' as a function of the Weber number, it is clear that there will be distinct solutions λ' for each m, with all the coupling modes (n) contributing to these solutions. Therefore, the technique will be to assign a value to m and to solve numerically the resulting infinite determinant. The analysis will be concerned mainly with the smaller values of n and m, because these deformations most nearly simulate those observed in experiments, and also because the surface tension, which maintains stability of the shape of the bubble, is much more dominant than the hydrodynamic pressure for the higher-order deformations (n large), as evidenced by the dependence on n^2 of the term due to surface tension in (20). Actually the modes $n = 1$, $m = 1$ and $n = 2$, $m = 1$ are most closely representative of the observed motion of the bubble once instability occurs.

C. *Numerical solution of equation* (20) *for asymmetric modes.*

It has not been possible to obtain a general solution of (20) in closed form. Indeed, there is no general theory available for the numerical solution of a five-term recursion relation. However, for the neutral point of the stability calculation $\lambda' = 0$, equation (20) reduces to a three-term recursion formula involving the Weber number and the a_{nm}. This relation

is analogous to the three-term recursion formula obtained in the calculation of the stability of the solutions of the Mathieu equation (Morse & Feshbach 1953, p. 557). There it is shown that the a_{nm} converge only for certain values of W^2 and a_{21}/a_{11}. These characteristic values are found by the method of continued fractions. This technique is the same as forming the determinantal equation from (20) with $\lambda' = 0$ and solving the resulting polynomial in W^2 for the characteristic values. Of course, the determinant contains an infinite number of terms for each value of m, but it is found that rapid convergence for the characteristic values W^2 is obtained by cutting off the determinant in successively larger segments. This process of cutting off the determinant is equivalent to terminating the continued fraction. The rapid convergence is to be attributed to the term $(n-1)(n+2)$ in (20) which predominates over the other coefficients which vary as n for large values of n for any given m. The results of this calculation give values of the critical Weber number for each m. To see that values of the Weber number smaller than this lead to stable solutions, the general equation (20) is solved by an analogous method to obtain a curve of λ'^2 *vs* W^2. It is found in expanding the determinants that only even powers of λ' occur, and further, regardless of the mode selected or order of the determinant included in the calculation, the values of λ'^2 are always real. That this should occur is suggested by the absence of any damping terms in the problem. From these facts it is clear that all solutions are either purely oscillatory ($\lambda'^2 < 0$) or purely divergent ($\lambda'^2 > 0$).

The critical Weber number calculated as described above, for $m = 1$, is 1·65. Figure 6 shows how λ'^2 varies with the Weber number as calculated from both the 2×2 and 4×4 determinants for $m = 1$. Going to higher order determinants gives results only negligibly different from those obtained from the 4×4 determinent. The amplitudes converge exceedingly rapidly.

The curves of figure 6 indicate the possibility of stable oscillations of the bubble in the lower modes for Weber numbers ranging from zero to critical. Of course, these oscillations are not observed in the experiments, since in this range the bubbles are seen to rise rectilinearly. This discrepancy may be explained by the absence of viscous effects in the theory. For Weber numbers of the order of unity to critical, the predicted values of λ'^2 vary from $-0{\cdot}5$ to $-0{\cdot}1$. Since the non-dimensionalizing factor in λ'^2 (i.e. $T/\rho R_0^3$) is of the order of $1{\cdot}5 \times 10^5$, the actual values of $i\lambda$ range from 250 to 120 approximately. This results in periods of oscillation between 0·025 sec and 0·05 sec, which corresponds to the time required for the average bubble to travel only four and eight bubble diameters, respectively. At these relatively high frequencies of oscillation, it may be expected that viscosity would damp the motion rather completely, since the theory developed by Rayleigh (see Lamb 1932, p. 640) may sensibly be applied. Consequently, the purely imaginary values of λ' encountered in the analysis are to be considered as representing stable motion of the bubble, with the possible exception of the points just short of the critical Weber number where λ' becomes equal to about $0{\cdot}01i$. Then, perhaps, viscosity would be less significant in damping the stable oscillations. However, since the

objective of the theoretical analysis is to calculate the Weber number at which the bubbles become unstable, it does not seem necessary to dwell on the question of whether the observed instability occurs for λ'^2 equal to $-0{\cdot}01$ or $+0{\cdot}01$. For Weber numbers above critical, the motion is a purely divergent, asymmetric one which presumably represents a darting motion of the bubble to one side of its original path. Motion pictures of unstable bubbles leaving an orifice with vegetable dye in their wakes indicate that the amplitude of the oscillation is several bubble diameters. This is indicative of a non-linear motion, or at least, a motion that could not be derived from small-perturbation techniques.

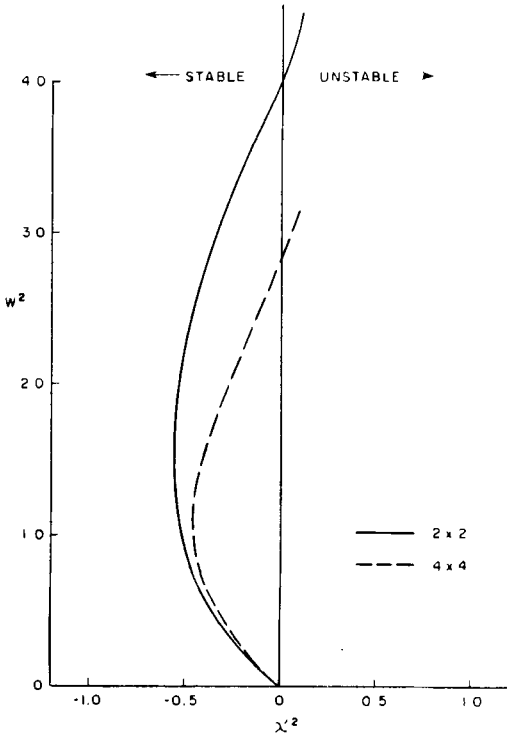

Figure 6. Theoretical stability curve.

To summarize the preceding paragraph, the predicted high-frequency steady oscillations of the bubble at small Weber numbers is interpreted to correspond to the steady rectilinear motion actually observed. The divergent motion predicted for Weber numbers above the critical value (or, what is equivalent, the slow steady oscillation predicted just below the critical W) is interpreted to represent the large-amplitude oscillatory motion actually observed in that regime.

In closing this section of the analysis, it is necessary to mention once again that only very slight steady-state deformation of the bubble was considered, consistent with the neglecting of the squares of the perturbation amplitudes. In practice, it is found that the sub-critical bubbles are somewhat more deformed in the shape of oblate spheroids than this calculation

may legitimately permit. This question will be considered in more detail in the following section. However, it may be said that the analysis presented here serves to explain qualitatively a possible mechanism for the instability of bubbles under the basic assumptions considered.

4. DEFORMATION OF BUBBLES AND ITS EFFECTS ON THE STABILITY

The deformation of bubbles from the spherical shape as they rise uniformly in an inviscid fluid under the action of the hydrodynamic pressure and surface tension may be calculated from the steady-state terms of the previous calculation (see (19)), at least to first order in the perturbation

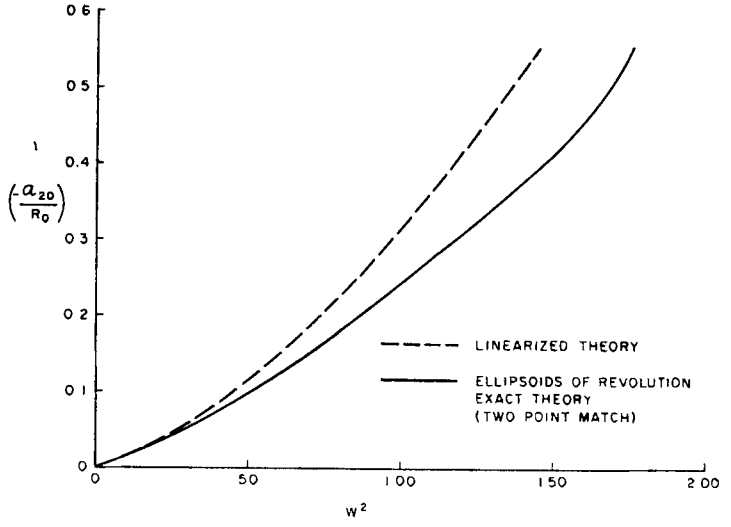

Figure 7. Bubble deformation calculated by approximate methods.

amplitudes. The relations for $p'_{(\lambda=0,\, m=0)}$ and $\tau'_{(\lambda=0,\, m=0)}$ may be calculated from (16). If the resulting system of linear, inhomogeneous algebraic equations is solved by Cramer's rule, one obtains

$$\frac{a_{20}}{R_0} \doteq \frac{3}{4}\frac{W^2(3{\cdot}58W^2-18)}{(5{\cdot}52W^4-43{\cdot}6W^2+72)}, \tag{22}$$

approximately. Again the infinite set of algebraic equations has been terminated and rapid convergence has been obtained. The ratio a_{20}/R_0 is a measure of the deformation of the sphere into an ellipsoid at various Weber numbers. Equation (22) is plotted in figure 7 (dashed line). That such large deformations in shape are predicted by the linear theory is, at first thought, quite alarming, for it places in question the application of the stability calculation of the previous section to gas bubbles rising in liquids. It is observed that just sub-critical bubbles are quite deformed in the experiments—almost as much as indicated by (22). Therefore the possible effect of ellipticity of the bubbles on the quantitative values of the stability criterion of the asymmetric modes will be dealt with in this section. It will be shown that the qualitative behaviour is not altered.

To obtain an estimate of higher-ordered effects in the deformation of a bubble in an inviscid fluid, one may start with the pressure distribution

about an oblate spheroid in such a fluid, and knowing the principal radii of curvature at the stagnation point ($\theta = 0$) and equator ($\theta = \pi/2$), simply require that the general equilibrium condition (17) be satisfied only at these points. The hydrodynamic pressure at the equator is given by

$$p = \tfrac{1}{2}\rho U^2 - \tfrac{1}{2}\rho U^2(1+k_a)^2, \tag{23}$$

where

$$k_a = (0{\cdot}622E - 0{\cdot}122) \tag{23 a}$$

and E is the ratio of semi-major to semi-minor axes (b/a). The values of k_a are tabulated in a paper by Zahm (1926). The sum of the reciprocals of the principal radii of curvature at the equator is $(b/a^2 + 1/b)$, while that at the stagnation point is $2a/b^2$. Therefore, for equilibrium,

$$p_i = \tfrac{1}{2}\rho U^2 + 2aT/b^2 \tag{24}$$

and

$$p_i = \tfrac{1}{2}\rho U^2 - \tfrac{1}{2}\rho U^2(1+k_a)^2 + T(b/a^2 + 1/b), \tag{24 a}$$

and since the gas pressure within the bubble (p_i) is uniform,

$$T(2a/b^2 - b/a^2 - 1/b) = -\tfrac{1}{2}\rho U^2(1+k_a)^2. \tag{25}$$

To maintain constant volume, we have

$$ab^2 = R_0^3, \qquad \text{i.e. } b = R_0 E^{1/3}. \tag{26}$$

The Weber number obtained by solving (25) and (26) is

$$W^2 = \frac{2}{E^{1/3}} \frac{(E^2 + 1 - 2/E)}{(1+k_a)^2}, \tag{27}$$

which gives the deformation of the bubbles as a function of the Weber number. Since the semi-minor axis of the spheroid is equal to $R_0/E^{2/3}$ and the amplitude ratio $a_{20}/R_0 \doteqdot (a/R_0 - 1)$, we may use the relation $a_{20}/R_0 \doteqdot (E^{-2/3} - 1)$ in conjunction with (27) to plot this latter equation adjacent to (22) in figure 7 (solid curve). The results show that (27) verifies the linearized theory for small Weber numbers, but gives smaller deformations for somewhat larger values.

The existence of distortion in the shape of the bubbles would make the perturbation of an oblate spheroid, rather than a sphere, seem a more reasonable attack on the problem of the stability of the bubbles. The equations, employing oblate spheroidal coordinates, have been derived. Though not amenable to complete solution immediately, this analysis further verifies the qualitative correctness of the theory developed for the sphere, and together with the 'two-point' calculation mentioned above, suggests a method for deriving better quantitative results from this theory. Briefly, this method consists in replacing the form $(3/2)U\sin\theta$ for the tangential velocity by the increased value appropriate to an oblate spheroid of any given eccentricity (Zahm 1926), in the boundary condition (5). If this is done, it is found that instead of having $9/4W^2$ equal to the characteristic value of (20) for the neutral stability point ($\lambda' = 0$), the square of the increased value replaces the coefficient 9/4. Thus, an improved estimate of critical Weber number may be obtained for any assumed deformation E (equal to the ratio of semi-major to semi-minor axes of the spheroid). But the appropriate

deformation is actually a function of Weber number, and may be estimated by the 'two-point' calculation. The consistent case is the one for which the critical Weber number is just that required to produce the assumed deformation. This turns out to be $E = 2{\cdot}20$, for which $W_{cr} = 1{\cdot}23$. This Weber number is in excellent agreement with the experimental value. Moreover, the deformation of bubbles in most of the pure, fast liquids just prior to instability, as estimated from photographs supplied by Haberman & Morton, is approximately given by $E = 2{\cdot}1$. An outstanding exception is provided by bubbles in the *filtered* water employed by these experimenters, where $E = 1{\cdot}5$. The present authors employing *double-distilled* water available commercially, obtained a deformation $E = 1{\cdot}75$.

It is suggested from the results of these approximate calculations that the deformation of the bubbles prior to oscillation reduces the value of the critical Weber number as calculated from the perturbation of an essentially spherical bubble, thus bringing it into better agreement with observations. Throughout this section it has been implied that the Weber-number effects are largely responsible for the actual deformation of the bubble; hence the present agreement with experimental results supports all previous experimental evidence in establishing the dominance of these effects for bubbles rising in the pure, fast liquids at Weber numbers near and somewhat beyond the critical value.

5. Conclusions

The conclusions derived from the experiments were listed at the end of § 2. From the theoretical analysis, the following conclusions may be drawn.

1. The results derived from the investigation of the stability of a deformable sphere in a uniform, inviscid, incompressible and irrotational flow by the perturbation of the shape of the sphere, indicate, at least qualitatively, that the interaction of surface tension and hydrodynamic pressure provides a possible mechanism of instability. In fact, in any situation where the deformable sphere is not subjected to considerable changes in shape just prior to the onset of instability, this analysis would be expected to give accurate quantitative results as well.

2. The agreement between the approximate theory and the experimental results for the steady-state deformation of the bubbles under the action of only hydrodynamic pressure and surface tension, for moderate values of the Weber number, provides additional evidence of the important roles played by these effects in the motion of bubbles in that range.

3. The inclusion of the effects of deformation of bubbles by approximate methods in the stability calculation of the nearly spherical bubble yields a critical Weber number of 1·23, which agrees well with the experimental value.

The authors wish to express their gratitude to Professors Nicholas Rott and Frank E. Marble for the helpful suggestions they contributed, and to the Office of Naval Research, which sponsored this research.

References

BRYN, T. 1949 Speed of rise of air bubbles in liquids, *David Taylor Model Basin, Translation* no. 132.

DATTA, R. L., NAPIER, D. H. & NEWITT, D. M. 1950 The properties and behaviour of gas bubbles formed at a circular orifice, *Trans. Instn Chem. Engrs.* **28,** 14–26.

DAVIES, R. M. & TAYLOR, G. I. 1950 The mechanics of large bubbles rising through extended liquids in tubes, *Proc. Roy. Soc.* A, **200,** 375–390.

GORODETSKAYA, A. 1949 The rate of rise of bubbles in water and aqueous solutions at great Reynolds numbers, *J. Phys. Chem. (Moscow)* **23,** 71–77 (in Russian).

HABERMAN, W. L. & MORTON, R. K. 1953 An experimental investigation of the drag and shape of air bubbles rising in various liquids, *David Taylor Model Basin, Rep.* no. 802.

HOEFER, K. 1913 Untersuchungen über die Stromungsvorgänge im Steigrohr eines Druckluft-Wasserhebers, *Mitt. ForschArb. Ingenieurw.* **138,** 1–12.

KAWAGUTI, M. 1955 The critical Reynolds number for the flow past a sphere, *J. Phys. Soc. Japan* **10,** 694–699.

LAMB, H. 1932 *Hydrodynamics.* 6th Ed. Cambridge University Press.

LANE, W. R. & GREEN, H. L. 1956 The mechanics of drops and bubbles; article in *Surveys in Mechanics,* Cambridge University Press.

MIYAGI, O. 1925 The motion of air bubbles rising in water, *Technol. Rep. Tohoku Univ.* **5,** 135–167.

MORSE, P. M. & FESHBACH, H. 1953 *Methods of Theoretical Physics.* New York: McGraw-Hill.

RICHARDSON, E. G. 1950 *Dynamics of Real Fluids.* London: Edward Arnold.

ROSENBERG, B. 1950 The drag and shape of air bubbles moving in liquids, *David Taylor Model Basin, Rep.* no. 727.

SAFFMAN, P. G. 1956 On the rise of small air bubbles in water, *J. Fluid Mech.* **1,** 249–275.

STUKE, B. 1952 Das Verhalten die Oberfläche von sich in Flüssigkeiten bewegenden Gasblasen, *Naturwissenschaften* **39,** 325–326.

ZAHM, A. F. 1926 Flow and drag formulas for simple quadrics, *Nat. Adv. Comm. Aero., Wash., Rep.* no. 253, 531.

Note added in proof

In discussion of the stability curve (figure 5) since submission of this paper, the question has been raised whether the horizontal ($W \doteqdot 1{\cdot}26$) and vertical ($Re \doteqdot 202$) branches of this curve should not be extended to the left and upward, respectively, from their point of intersection. In answer to this question, the authors point out that neither they nor other experimenters have observed oscillations in these regions of the diagram. As a bubble rises from rest in a liquid, its instantaneous Weber and Reynolds numbers trace a curve that rises toward the right from the origin in figure 5, its steepness depending on the fluid properties. For the experimental points plotted in figure 5, a Reynolds-number-dependent fluid produces instability when this curve crosses $Re \doteqdot 202$; a Weber-number-dependent fluid does not cause instability as the curve crosses this branch, but only where it reaches $W \doteqdot 1{\cdot}26$. The ' more viscous liquids ' mentioned on page 28 seem to be those whose trajectory curves rise to the left of the point (202, 1·26) in figure 5, and, as mentioned, these do not exhibit instability at all. To be sure, there are only a few data on these liquids; nevertheless, the extrapolation of the horizontal and vertical branches of the stability curve must be considered unwarranted at present.